

Synthesis of Polypyrrole-coated NiO/Ni(OH)₂ Hybrid Flowers Composite by Pulse Electro-polymerization for supercapacitor with Improved Electrochemical Capacitance

Ji Yan^{1,*}, Serubbabel Sy², Heng Wang¹, Yong Zhang^{1,*}, Ai-Ping Yu³, Li-Zhen Wang^{1,*}, Li-Ming Zhou¹

¹ School of Material and Chemical Engineering, Henan Provincial Key Laboratory of Surface Interface Science, Zhengzhou University of Light Industry, Zhengzhou 450001, Henan, China

² Department of Chemical Engineering, Waterloo Institute for Nanotechnology, Waterloo Institute for Sustainable Energy, University of Waterloo, Canada

*E-mail: jiyan@zzuli.edu.cn, wlz@zzuli.edu.cn

Received: 1 February 2020 / Accepted: 21 September 2020 / Published: 31 October 2020

This work describes a novel strategy to synthesize polypyrrole-coated NiO/ α -Ni(OH)₂ hybrid flower with an improved capacitance performance for supercapacitor. Polypyrrole nanoparticles with a size of 80-100 nm were prepared by a pulse electro-polymerization and uniformly embedded into the petal gap of the self-assembled NiO/ α -Ni(OH)₂ hybrid flower. Due to the enhancement of the electrical conductivity and the improvement of electrochemical pseudo-capacitance, the as-synthesized polypyrrole-coated NiO/ α -Ni(OH)₂ hybrid flower composite showed a high reversible specific capacity of 359 F g⁻¹ at 5 A g⁻¹ in 2 M KOH electrolyte in a potential range of 0 - 0.45 V. Benefiting from the unique electro-polymerization design, the obtained hybrid flower composite demonstrated excellent capacitive performance and cycling stability after 1000 cycles, demonstrating the promising application as a high-performance pseudocapacitive material for supercapacitors.

Keywords: Supercapacitors, Polypyrrole, Hybrid flower, Pulse electro-polymerization

1. INTRODUCTION

With the tremendous development of electric vehicle, finding a suitable energy storage device to combine the advantages of high power density of supercapacitors and high energy density of lithium ion batteries, has attracted much attention from worldwide researchers [1]. Pseudocapacitor, as one of the promising electrochemical storage candidates, shows a lot of merits, including high power density, low maintenance cost and long cycling life. However, the relatively low energy density of pseudocapacitor compared with lithium ion batteries has severely limited its further application in electric vehicle. Although traditional transition metal oxides, such as RuO₂ and IrO₂, have been investigated extensively

as potential electrode materials in pseudocapacitor because of the high capacitance of 1580 F g^{-1} and 550 F g^{-1} , respectively, the high cost and toxic have still hampered their commercial application. Considering this aspect, a broad range of alternative materials with low cost and excellent performance, such as nickel oxide [2,3], cobalt oxide [4,5], manganese dioxide [6,7] and nickel cobalt oxide [8], have been widely investigated. Among these materials, nickel oxide (NiO) with a specifically theoretical capacitance of 2573 F g^{-1} has been considered as the most promising electrode material by the virtue of low cost and environmentally benign nature [9-13]. However, the practical application of NiO in pseudocapacitor has been hindered by its poorly intrinsic electronic conductivity. Up to now, various of methods for improving the electronic conductivity of NiO have been explored, such as surface coating or physical mixing with carbon support [14]. Based on our previous report [15], we had successfully prepared a flower-structured NiO/ α -Ni(OH)₂ hybrid composite by using a solvothermal method followed a tailoring calcination process. The hybrid composite exhibits a superior capacitance than pure NiO and Ni(OH)₂ individually.

Alternatively, polypyrrole (PPy), as an important kind of conductive polymers, has been introduced as a reasonable matrix for improving the capacitance [16], optical property [17] and lithium storage ability of transition metal oxides [18] owing to its attractive advantages of high electrical conductivity ($\gg 1 \text{ S cm}^{-1}$), environmental compatibility, and easy preparation route. Through mixing or coating with PPy has been proven as an effective method to increase the electronic conductivity and to further enhance the electrochemical performance of NiO.

In this study, PPy nanoparticles-coated NiO/ α -Ni(OH)₂ hybrid flower composite has been firstly synthesized by a pulse electro-polymerization and the effect of the PPy-pulse-polymerized time on the capacitance of the hybrid composite was investigated.

2. EXPERIMENTAL

2.1. Preparation of PPy-coated NiO/ α -Ni(OH)₂ hybrid flower

The NiO/ α -Ni(OH)₂ hybrid flower composites were prepared by a solvothermal method reported previously [15]. 0.582 g Ni(NO₃)₂·6H₂O, 1.20 g urea and 0.10 sodium dodecyl sulfate (SDS) were dissolved into a mixture solution (10 ml double deionized water (DDI water) and 10 ml ethanol) and magnetically stirred at room temperature until a homogeneous light-green solution was obtained. Then, the solution was transferred into a Teflon-lined stainless-steel autoclave, where the solution was heated at 110°C for 15 h in an air-flow oven. After heating, the obtained product was washed with DDI water for three times and acetone for two times. Once drying the washed product at 60°C for one night, the light-green precursor powder was further sintered at 250°C for 40 min in air to synthesize NiO/ α -Ni(OH)₂ hybrid flower composite.

For the preparation of PPy nanoparticle-coated NiO/ α -Ni(OH)₂ hybrid flower composite, a solution of as-prepared NiO/ α -Ni(OH)₂ hybrid composite was ultra-sonicated for 20 min, drew 20 μl solution and coated on a glassy carbon electrode with a diameter of 5 mm. After drying at 30°C for 20 min, the electrode was immersed into a 1 M KCl solution and 5 mM pyrrole (Py) monomer solution was

used as polymer raw material for pulse electro-polymerization. A three electrode system consisting of a platinum (Pt) wire as the counter electrode and a saturated calomel electrode (SCE) as the reference was adopted to coat PPy spots on the surface of NiO/ α -Ni(OH)₂ hybrid flower composite [19].

2.2. Materials Characterization

The morphology and microstructure of as-synthesized composites were observed with a field emission scanning electron microscopy (SEM, LEO FESM 1530.20V).

2.3. Electrochemical Characterization

All electrochemical measurements were also conducted in the same three electrode system. The as-synthesized sample was served directly as the working electrode, and a Pt wire electrode and a SCE were used as the counter electrode and the reference electrode, respectively. 2 M KOH was used as electrolyte. The preparation procedure of the working electrode was the same step as that of our previous literature [15].

Cyclic voltammetry (CV) was performed using a VERSASTAT mc potentiostat from Princeton Applied Research. The potential varied from 0 to 0.45V versus SCE.

3. RESULTS AND DISCUSSION

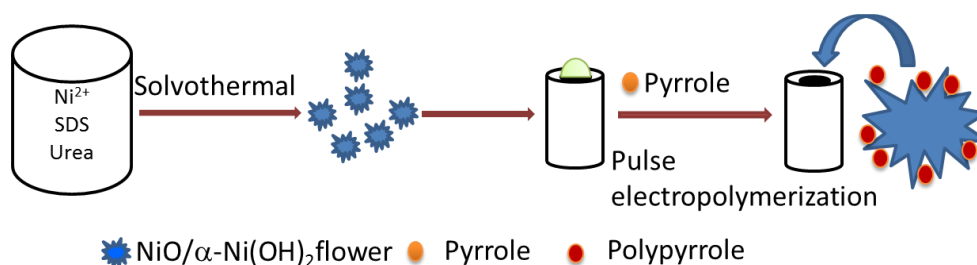


Figure 1. Scheme of pulse electro-polymerization of polypyrrole nanoparticle onto NiO/ α -Ni(OH)₂ hybrid flower.

Fig.1 illustrates the synthesis procedure of polypyrrole nanoparticle-coated NiO/ α -Ni(OH)₂ hybrid flower. The synthesis process of NiO/ α -Ni(OH)₂ flower is as same as that of our previous report [15]. After obtaining the special flower morphology, we prepared the ink solution and dropped 20 μl of the dispersed solution onto a 5 mm OD glassy carbon. With drying the electrode, we used the NiO/ α -Ni(OH)₂ flower coated glassy carbon as the working electrode, a Pt wire as the counter electrode and a SCE as the reference electrode. Pulse electro-polymerization method was applied to coat polypyrrole nanoparticle onto the petal gap of the NiO/ α -Ni(OH)₂ hybrid flower.

Fig. 2 shows SEM images portraying the morphology of bare NiO/ α -Ni(OH)₂ hybrid flower (NOF 0s) and PPy nanoparticle-coated NiO/ α -Ni(OH)₂ hybrid flower (NOF-PPy 80s). As illustrated in Fig.2 (a) and (b), the NOF 0s mainly consists of flower-like hierarchical structure with particle size ranging from 0.5 to 2 μ m. However, for NOF-PPy 80s sample, we can clearly see that the petal gaps of flower-like surface of NiO/ α -Ni(OH)₂ is partly decorated with some small PPy nanoparticles (as shown in Fig. 2 (c) and (d)). The average size of the PPy particles is about or less than 100 nm.

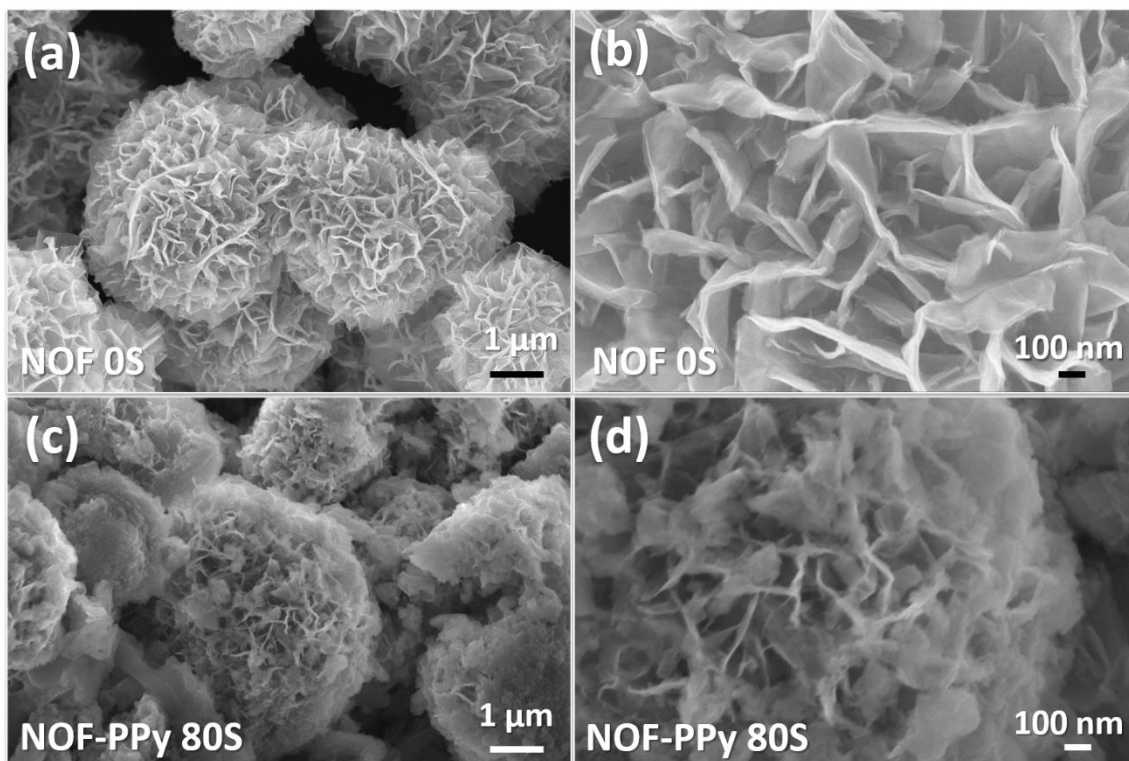
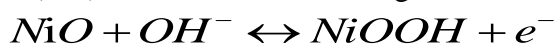


Figure 2. SEM images of (a, b) NOF 0s, and (c, d) NOF-PPy 80s.

In order to investigate the effect of PPy nanoparticles decoration on the capacitance of the NiO/ α -Ni(OH)₂ flower, CV curves of NOF 0s and NOF-PPy 80s were obtained at a 5 mV s⁻¹ and a 100 mV s⁻¹ scanning rate in the potential range of 0 - 0.45 V (vs SCE), as shown in Fig. 3. As can be seen, both CV curves exhibit clear redox peaks, indicating the significantly typical pseudocapacitive behavior of NiO/ α -Ni(OH)₂ based on the following surface Faradic reaction [20-23]:



Compared with the NOF 0s electrode, the NOF-PPy 80s electrode delivers almost the same value of capacitance (240.1 F g⁻¹) at 5 mV s⁻¹ (Fig. 3(a)) but much higher capacitance at 100 mV s⁻¹ (Fig. 3(b)), which means the PPy making more contribution to the electronic conductivity at a higher scanning rate since the relatively high electronic conductivity [24]. The specific capacitance of the NOF-PPy 80s electrode researches 240.0 F g⁻¹ and 134.5 F g⁻¹ at 5 mV s⁻¹ and 100 mV s⁻¹, respectively. For both electrodes, the equivalent value of specific capacitance at 5 mV s⁻¹ may come from the relatively lower theoretical capacitance of PPy (620 F g⁻¹ under doping state) [25] than that of NiO [26] or α -Ni(OH)₂

[27]. When increasing the scanning rate to 100 mV s^{-1} , PPy nanoparticles with a high electronic conductivity play more critical role in enhancing the specific capacitance of the hybrid composite than that at a low scanning rate (5 mV s^{-1}).

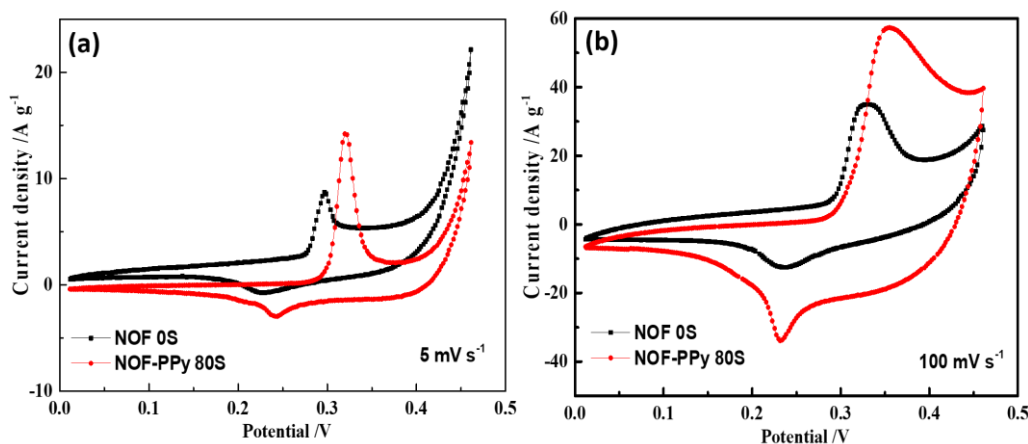


Figure 3. CV curves of NOF 0s and NOF-PPy 80s: (a) at 5 mV s^{-1} , (b) at 100 mV s^{-1} .

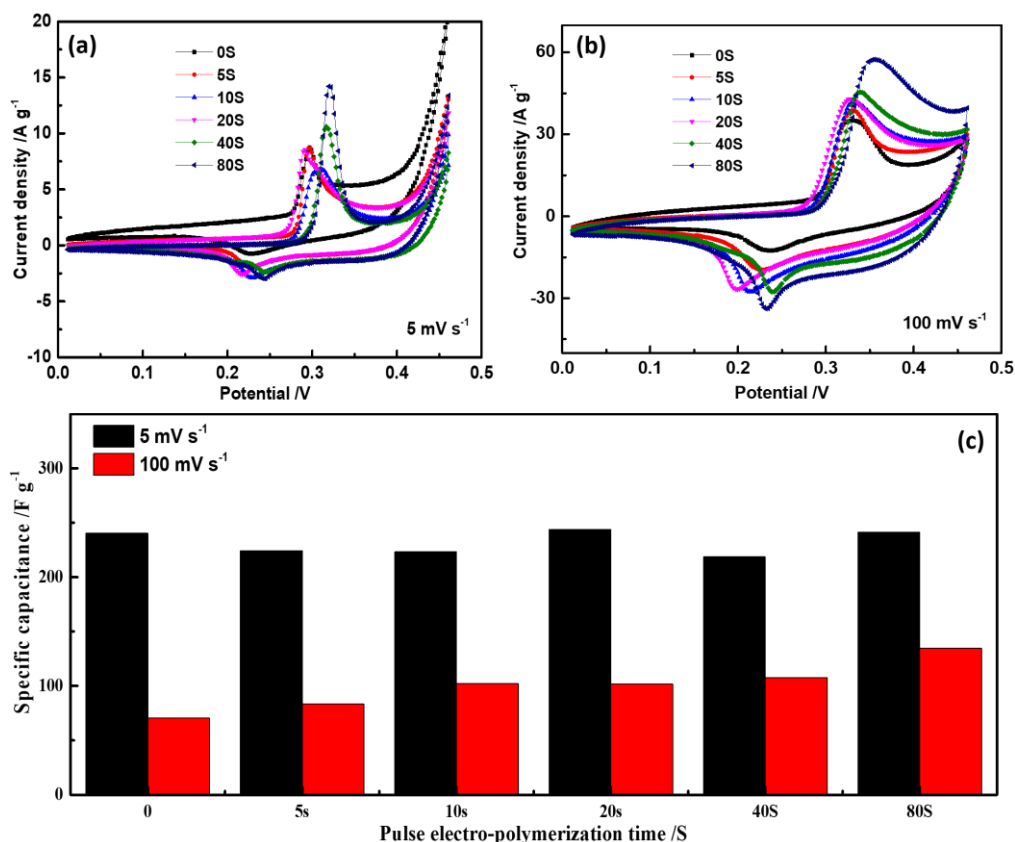


Figure 4. CV curves of NOF 0s (0s) and PPy nanoparticles-coated $\text{NiO}/\alpha\text{-Ni(OH)}_2$ hybrid flower with various pulse electro-polymerization time (5s, 10s, 20s, 40s, 80s) (a) at 5 mV s^{-1} , and (b) at 100 mV s^{-1} ; (c) average specific capacitance at different pulse electro-polymerization time (Black column value corresponds to 5 mV s^{-1} scanning rate while red column value corresponds to 100 mV s^{-1}).

CV curves of the NOF 0s electrode and the PPy nanoparticles-coated NiO/ α -Ni(OH)₂ hybrid flower electrodes with various pulse electro-polymerization time (5s, 10s, 20s, 40s, 80s) are shown in Fig. 4 (a) and (b) at 5 mV s⁻¹ and 100 mV s⁻¹, respectively. From the profiles, we can see that the oxidation and reduction peaks of all NiO/ α -Ni(OH)₂ based composites almost keep the same shape, suggesting the suitable coating PPy does not affect the electrochemically capacitive behavior of NiO/ α -Ni(OH)₂. It is noted that all specific capacitance of PPy coated composites retain the same value as that of NOF 0s electrode at 5 mV s⁻¹, which further confirms that the surface area of the active material is not the solely key factor [28]. However, when increasing the scan rate from 5 mV s⁻¹ to 100 mV s⁻¹, the electronic conductivity has become the controllable factor in determining the electrochemical properties of active material, as shown in Fig. 4(c). The further research work is still running and we will report it in the next paper once we get reasonable results.

The specific capacitances are shown in Fig. 5 as a function of a cycling number. We can see that the initially specific capacitance of NOF 0s reaches 104.8 F g⁻¹ while NOF-PPy 80s shows 299.5 F g⁻¹ at a current density of 5 A g⁻¹. After activation in the initial 20 cycles, the NOF-PPy 80s possesses a specific capacitance of 359 F g⁻¹, which is much higher than that of NOF 0s (155 F g⁻¹). The high capacitance of NOF-PPy 80s could be attributed to the suitable polypyrrole amount deposited on the surface of NiO/ α -Ni(OH)₂, which not only provides an improved electronic conductivity but also makes contribution to the transformation of Ni(OH)₂ to NiO [15]. After 1000 cycles, the NOF-PPy 80s electrode still maintains a specific capacitance of 169.8 F g⁻¹, higher than that of NOF 0s (104.8 F g⁻¹) even there is a capacitance decay in the initial 600 cycles.

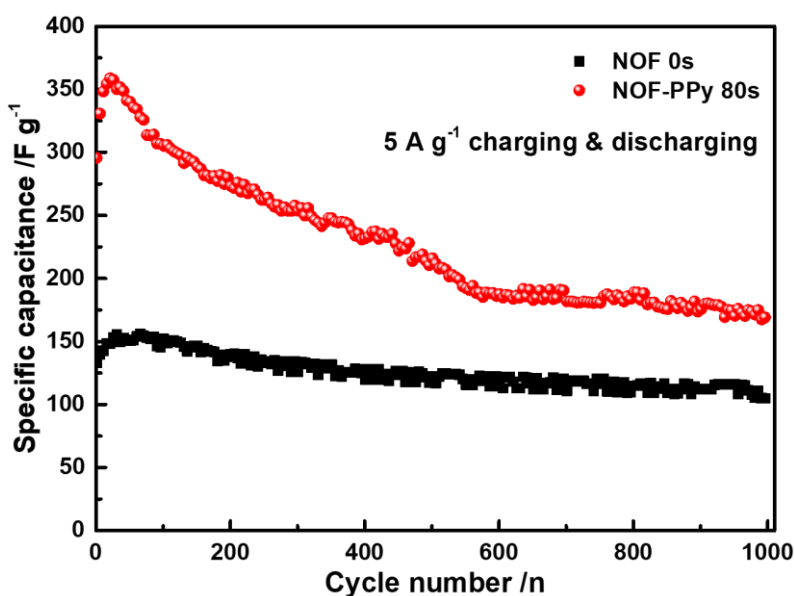


Figure 5. The electrochemically cycling stability of NOF 0s and NOF-PPy 80 s at 5 A g⁻¹ current density.

The pulse electro-polymerization, which is different from traditionally continuous electro-polymerization, gives enough time for pyrrole monomers in the immediate vicinity of the petal and precipitated on the surface of NiO/ α -Ni(OH)₂ [29]. Such electro-polymerization strategy facilitates the

considerable consumption of all remained deposition current, which results in the rare nucleation of new PPy chains on the NiO/ α -Ni(OH)₂ petal surface to enlarge the polymer particles and ensure the little penetration into the porous network of NiO/ α -Ni(OH)₂ [30]. Although the capability of NOF-PPy 80 s is lower than that of other samples, a maximum specific capacitance of 360 F g⁻¹ is achieved at a current density of 5 A g⁻¹. Such the capacitance is comparable to other NiO-based or conductive polymer-based composite electrodes (**Table 1**), indicating the obtained PPy nanoparticle-coated NiO/ α -Ni(OH)₂ possesses an excellent electrochemical capacitive storage performance and could be used as an ideal electroactive materials in supercapacitors.

Table 1. Electrochemical properties comparison between this work and literatures.

Electrode	Electrolyte	Current density	Capacitance	References
NiO/PPy	2 M KOH	5 A g ⁻¹	358 F g ⁻¹	This work
NiO/EG-60	6 M KOH	0.1 A g ⁻¹	486 F g ⁻¹	[31]
NiO-PANI/Carbon cloth	0.5 M H ₂ SO ₄	0.5 A g ⁻¹	192.3 F g ⁻¹	[32]
NiO-PANI	1 M H ₂ SO ₄	5 A g ⁻¹	417 F g ⁻¹	[33]
NiO-PANI	1 M H ₂ SO ₄	1 A g ⁻¹	362 F g ⁻¹	[34]
NiO-SG	6 M KOH	5 A g ⁻¹	307 F g ⁻¹	[35]
MoS ₂ /PPy	1 M KCl	1 A g ⁻¹	307.5 F g ⁻¹	[36]
Ni ₂ P/PPy	1 M Na ₂ SO ₄	1 A g ⁻¹	476.5 F g ⁻¹	[37]

Electrochemical impedance spectra of NOF 0s and NOF-PPy 80s was further carried out with a signal amplitude of 10 mV versus SCE within a frequency range of 100 kHz to 10 mHz in 2M KOH and the results are shown in Fig. 6. As shown, both electrodes demonstrate similar shape, which is composed of a semicircle and a liner at low-frequency region [38]. The semicircle corresponds to the charge transfer resistance in high-frequency region while the liner represents the electrolyte diffusion resistance [39]. From the expanded spectra, the similarly charge transfer resistance of NOF 0s (5.01 Ω) and NOF-PPy 80s (4.98 Ω) indicates the uniform dispersion of ink during the preparation and the well-technology of drop coating on OD glass carbon. Simultaneously, the low charge transfer resistance suggests the improved reaction activity and electrochemical capacitance. The slight large slope at the low-frequency area reveals a low diffusion resistance and rapid ion diffusion between electrolyte interface and active materials.

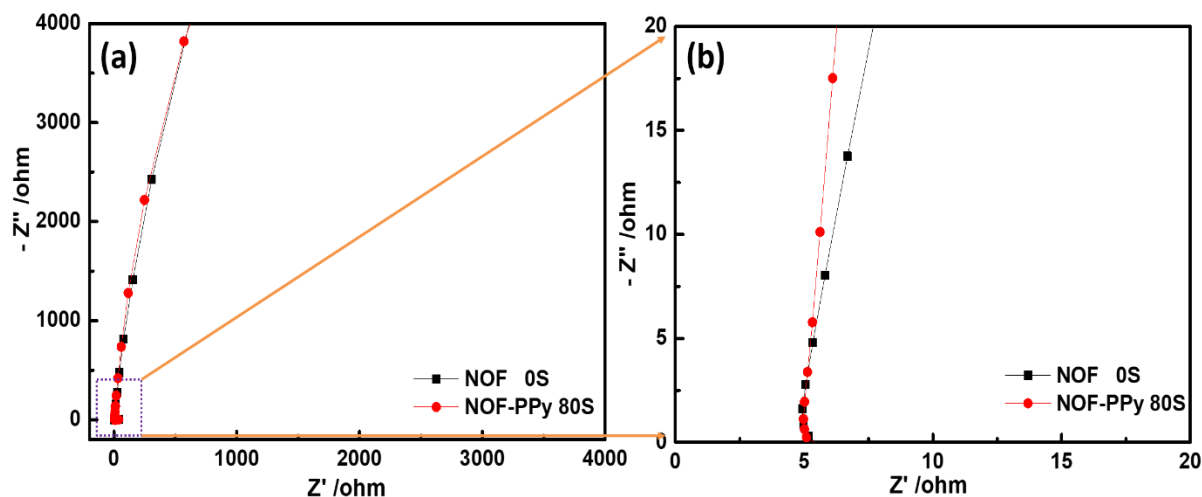


Figure 6. (a) Nyquist plots of NOF 0s and NOF-PPy 80s; (b) the expanded area of the red region marked in the Nyquist plots.

Based on above analysis, NiO/ α -Ni(OH)₂ hybrid flower coated with PPy nanoparticles can be successfully synthesized by a pulse electro-polymerization strategy. With the surface decoration with PPy, an enhanced electrochemical capacitance with superior rate capability was obtained. The possible reason of such improvement can be attributed to: 1) the high conductivity of PPy basically decreases the charge-transfer resistance during the electrochemically pseudocapacitive reaction, especially at a high scan rate/current density; 2) The unique merits of pulse electro-polymerization ensures all consumption of the applied current on the petal of NiO/ α -Ni(OH)₂; This strategy facilitates the rare nucleation of new PPy chains on the surface of NiO/ α -Ni(OH)₂ petal to enlarge the polymer particles, and ensures the little penetration of electrolyte into the porous network of NiO/ α -Ni(OH)₂; and 3) more reactive sites provided by PPy also makes contribution to the electrochemical kinetics.

4. CONCLUSION

In summary, polypyrrole nanoparticle-coated NiO/ α -Ni(OH)₂ hybrid flower composite has been successfully synthesized by a solvothermal process followed pulse electro-polymerization. Nano-size polypyrrole particles with 80-100 nm were embedded into the petal gap of NiO/ α -Ni(OH)₂ hybrid flower and the polypyrrole nanoparticle-coated NiO/ α -Ni(OH)₂ sample with 80s pulsing electro-polymerization time shows 359 F g⁻¹ of specific capacitance at a 5 A g⁻¹ current density. Additionally, the as-prepared composite also shows good capacitance rate retention when increasing the scan rate from 5 mV s⁻¹ to 100 mV s⁻¹. The improved electrochemical properties of polypyrrole nanoparticle-coated NiO/ α -Ni(OH)₂ are primarily attributed to the synergistic effect of NiO/ α -Ni(OH)₂ with high pseudocapacitive value and surface coated PPy with highly electronic conductivity.

ACKNOWLEDGEMENT

This work was financially supported by the Key R&D and Promotion Projects in Henan Province (No. 192102210079), the basic research project of the Key scientific research project of the higher education institutions of Henan Province of China (Grant No. 20ZX008), and Doctoral foundation of Zhengzhou University of Light Industry (No. 2017BSJJ043). The authors also thank the financial support from the Natural Sciences and Engineering Research Council of Canada (NSERC), the University of Waterloo and the Waterloo Institute for Nanotechnology.

References

1. G.C. Li, Z.W. Yang, Z.L. Yin, H.J. Guo, Z.X. Wang, G.C. Yan, Y. Liu, L.J. Li, J.X. Wang, *Journal of Materials Chemistry A*, 7 (2019) 15541-15563.
2. J.H. Xu, L. Wu, Y. Liu, J.F. Zhang, J.M. Liu, S.S. Shu, X. Kang, Q.G. Song, D. Liu, F. Huang, Y. Hu, *Surfaces and Interfaces*, 18 (2020) 100420.
3. X.D. Guo, K.F. Yan, F.Y. Fan, Y.P. Zhang, Y.Q. Duan, J.L. Liu, *Materials Letters*, 240 (2019) 62-65.
4. D.F. Qiu, X. Ma, J.D. Zhang, B. Zhao, Z.X. Lin, *Chemical Physics Letters*, 710 (2018) 188-192.
5. G.Y. Lin, Y.L. Jiang, C.G. He, Z.Y. Huang, X.F. Zhang, Y.K. Yang, *Dalton Transactions*, 48 (2019) 5773-5778.
6. X. Bai, D.X. Cao, H.Y. Zhang, *Inorganic Chemistry Frontiers*, 7 (2020) 411-420.
7. H.H. Zeng, B.L. Xing, C.T. Zhang, L.J. Chen, H.H. Zhao, X.F. Han, G.Y. Yi, G.X. Huang, C.X. Zhang, Y.J. Cao, *Energy & Fuels*, 34 (2020) 2480-2491.
8. S. Zheng, Y.L. Song, S.X. Wang, L.Z. Wang, J. Yan, *Results in Physics*, 14 (2019) 102441.
9. R. S. Kate, S.A. Khalate, R.J. Deokate, *Journal of Alloys and Compounds*, 734 (2018) 89-111.
10. Y.F. Zhang, M. Park, H.Y. Kim, S.J. Park, *Journal of Colloid and Interface Science*, 500 (2017) 155-163.
11. S. Vijayakumar, S. Nagamuthu, G. Muralidharan, *ACS Applied Materials & Interfaces*, 5 (2013) 2188-2196.
12. X.X. Meng, J.Y. Li, B.L. Yang, Z.X. Li, *Applied Surface Science*, 507 (2020) 145077.
13. H.K. Jung, S.J. Lee, D.W. Han, A.R. Hong, H. S. Jang, S.H. Lee, J.H. Mun, H.J. Lee, S.H. Han, D.J. Yang, D.H. Kim, *Electrochimica Acta*, 330 (2020) 135203.
14. J.L. Lv, Z.Q. Wang, H. Miura, *Solid State Communications*, 269 (2018) 45-49.
15. B.K. Kim, V. Chabot, A. Yu, *Electrochimica Acta*, 109 (2013) 370-380.
16. J. Tao, N. Liu, L. Li, J. Su, Y. Gao, *Nanoscale*, 6 (2014) 2922-2928.
17. R. Brooke, J. Edberg, D. Landolo, M. Berggren, X. Crispin, I. Engquist, *Journal of Materials Chemistry C*, 6 (2018) 4663-4670.
18. Q. Liu, Y. Luo, W.L. Chen, Y.W. Yan, L.H. Xue, W.X. Zhang, *Chemical Engineering Journal*, 347 (2018) 455-461.
19. A. Davies, P. Audette, B. Farrow, F. Hassan, Z. Chen, J.-Y. Choi, A. Yu, *The Journal of Physical Chemistry C*, 115 (2011) 17612-17620.
20. H.K. Jung, S.J. Lee, D. Han, A. Hong, H.S. Jang, S.H. Lee, J.H. Mun, H. Lee, S.H. Han, D. Yang, D.H. Kim, *Electrochimica Acta*, 330 (2020) 135203.
21. J.H. Xu, L. Wu, Y. Liu, J.F. Zhang, J.M. Liu, S.S. Shu, X. Kang, Q.G. Song, D. Liu, F. Huang, Y. Hu, *Surface and Interfaces*, 18 (2020) 100420.
22. J.L. Lv, Z.Q. Wang, H. Miura, *Solid State Communications*, 269 (2018) 45-49.
23. P.B. Liu, M.Y. Yang, S.H. Zhou, Y. Huang, Y.D. Zhu, *Electrochimica Acta*, 294 (2019) 383-390.
24. M.Y. Zhang, Y. Song, D. Guo, D. Yang, X.Q. Sun, X.X. Liu, *Journal of Materials Chemistry A*, 7 (2019) 9815-9821.
25. J. Ren, R.P. Ren, Y.K. Lv, *Chemical Engineering Journal*, 349 (2018) 111-118.

26. X.Y. Hou, X.L. Yan, X. Wang, Q.G. Zhai, *Journal of Solid State Chemistry*, 263 (2018) 72-78.
27. L. Aguilera, Y. Leyet, R. Pena-Garcia, E. Padron-Hernandez, R.R. Passos, L.A. Pocrifka, *Chemical Physics Letters*, 677 (2017) 75-79.
28. J. Yan, R. Tjandra, H. Fang, L.X. Wang, A.P. Yu, *Diamond and Related Materials*, 89 (2018) 114-121.
29. A.M. Obeidat, M.A. Gharaibeh, M. Obaidat, *Journal of Energy Storage*, 13 (2017) 123-128.
30. S.L. Liu, Y. Chen, J. Ren, Y.Y. Wang, W. Wei, *Journal of Solid State Electrochemistry*, 23 (2019) 3409-3418.
31. J. Xu, X.F. Gu, J.Y. Cao, W.C. Wang, Z.D. Chen, *Journal of Solid State Electrochemistry*, 16 (2012) 2667-2674.
32. S.A. Razali, S.R. Majid, *Materials and Design*, 153 (2018) 24-35.
33. B.S. Singu, S. Palaniappan, K.R. Yoon, *Journal of Applied Electrochemistry*, 46 (2016) 1039-1047.
34. M. V, D. H, *Materials Today; Proceedings*, 5 (2018) 23148-23155.
35. L. Wang, H. Tian, D.H. Wang, X.J. Qin, G.J. Shao, *Electrochimica Acta*, 151 (2015) 407-414.
36. C.S. Chang, X.N. Yang, S.S. Xiang, H.A. Que, M. Li, *Journal of Materials Science: Materials in Electronics*, 28 (2017)1777-1784.
37. S.L. Liu, Y. Chen, J. Ren, Y.Y. Wang, W. Wei, *Journal of Solid State Electrochemistry*, 23 (2019) 3409-3418.
38. J. Yan, Y.Y. Fang, S.W. Wang, S.D. Wu, L.X. Wang, Y. Zhang, H.W. Luo, Y. Cao, H.L. Gao, L.Z. Wang, *International Journal of Electrochemical Science*, 15 (2020) 1982-1995.
39. Y. Ouyang, R.J. Huang, X.F. Xia, H.T. Ye, X.Y. Jiao, L. Wang, W. Lei, Q.L. Hao, *Chemical Engineering Journal*, 355 (2019) 416-427.

© 2020 The Authors. Published by ESG (www.electrochemsci.org). This article is an open access article distributed under the terms and conditions of the Creative Commons Attribution license (<http://creativecommons.org/licenses/by/4.0/>).